Received: 26 October 2022 | Revised: 22 December 2022 | Accepted: 29 December 2022

DOI: 10.1111/gcb.16595

Global Change Biology WILEY

RESEARCH ARTICLE

The detection and attribution of extreme reductions in vegetation growth across the global land surface

Hui Yang[1,2] | Seth M. Munson[3] | Chris Huntingford[4] | Nuno Carvalhais[1,5,6] | Alan K. Knapp[7] | Xiangyi Li[2] | Josep Peñuelas[8,9] | Jakob Zscheischler[10] | Anping Chen[7]

[1]Department of Biogeochemical Integration, Max Planck Institute for Biogeochemistry, Jena, Germany

[2]College of Urban and Environmental Sciences, Sino-French Institute for Earth System Science, Peking University, Beijing, China

[3]Southwest Biological Science Center, U.S. Geological Survey, Arizona, Flagstaff, USA

[4]U.K. Centre for Ecology and Hydrology, Oxfordshire, Wallingford, UK

[5]Departamento de Ciências e Engenharia do Ambiente, Faculdade de Ciências e Tecnologia, Universidade Nova de Lisboa, Caparica, Portugal

[6]ELLIS Unit Jena, Jena, Germany

[7]Department of Biology and Graduate Degree Program in Ecology, Colorado State University, Colorado, Fort Collins, USA

[8]CREAF, Catalonia, Barcelona, Spain

[9]CSIC, Global Ecology Unit CREAF-CSIC-UAB, Catalonia, Barcelona, Spain

[10]Department of Computational Hydrosystems, Helmholtz Centre for Environmental Research – UFZ, Leipzig, Germany

Correspondence
Anping Chen, Department of Biology and Graduate Degree Program in Ecology, Colorado State University, Fort Collins, Colorado, USA.
Email: anping.chen@colostate.edu

Hui Yang, Department of Biogeochemical Integration, Max Planck Institute for Biogeochemistry, Jena, Germany.
Email: huiyang@bgc-jena.mpg.de

Funding information
German Federal Ministry of Economics and Technology, Grant/Award Number: 50EE1904; National Natural Science Foundation of China, Grant/Award Number: 41988101; U.S. Department of Energy, Grant/Award Number: DE-SC0022074; MCIN, Grant/Award Number: TED2021-132627B-I00; European Union NextGenerationEU/PRTR

Abstract

Negative extreme anomalies in vegetation growth (NEGs) usually indicate severely impaired ecosystem services. These NEGs can result from diverse natural and anthropogenic causes, especially climate extremes (CEs). However, the relationship between NEGs and many types of CEs remains largely unknown at regional and global scales. Here, with satellite-derived vegetation index data and supporting tree-ring chronologies, we identify periods of NEGs from 1981 to 2015 across the global land surface. We find 70% of these NEGs are attributable to five types of CEs and their combinations, with compound CEs generally more detrimental than individual ones. More importantly, we find that dominant CEs for NEGs vary by biome and region. Specifically, cold and/or wet extremes dominate NEGs in temperate mountains and high latitudes, whereas soil drought and related compound extremes are primarily responsible for NEGs in wet tropical, arid and semi-arid regions. Key characteristics (e.g., the frequency, intensity and duration of CEs, and the vulnerability of vegetation) that determine the dominance of CEs are also region- and biome-dependent. For example, in the wet tropics, dominant individual CEs have both higher intensity and longer duration than non-dominant ones. However, in the dry tropics and some temperate regions, a longer CE duration is more important than higher intensity. Our work provides the first global accounting of the attribution of NEGs to diverse climatic extremes. Our analysis has important implications for developing climate-specific

disaster prevention and mitigation plans among different regions of the globe in a changing climate.

KEYWORDS
climate extremes, coincidence analysis, drought, flood, frost, heatwave, vegetation growth anomaly

1 | INTRODUCTION

Vegetation growth, indicated by satellite or tree ring proxies, is a key variable signifying the quantity and quality of essential ecosystem services such as carbon sequestration, mitigation of anthropogenic climate change and the provision of food and fibre for human consumption. Yet, vegetation growth is known to vary from year to year (Pappas et al., 2017). While small variations are expected and do not raise concerns, large and extreme negative anomalies in vegetation growth could lead to severely impaired ecosystem services (Felton, 2021; Piao et al., 2019; McDowell et al., 2020). Surprisingly, while reports of extreme negative anomalies of vegetation growth (NEGs) such as massive crop failure and tree mortality are often noted in the media (Hartmann et al., 2018; Lesk et al., 2016), we still lack a comprehensive assessment of them over broad scales (e.g., continental or global). Such understanding is critically important for both ecosystem science and public-policy decisions (Zscheischler et al., 2013).

Most of the research on "extremes" focuses on evaluating *climate* extremes (CEs) and their potential impacts given the more frequent and more severe contemporary CEs (e.g., Gampe et al., 2021; Overland & Wang, 2021). Reciprocally, we argue that a *vegetation*-oriented analysis seeking to evaluate and attribute different NEGs to different causes could complement the widely used climate-oriented approach and deepen our understanding of the causes and consequences of extreme vegetation responses. Extreme negative anomalies of vegetation growth are frequently associated with CEs (Frank et al., 2015), although other large-scale direct anthropogenic activities such as deforestation and logging have also contributed. However, the dominant cause of climate-driven NEGs still remains vague at regional and global scales, likely because a broad range of CEs and their combinations have potential to damage plants, while different biomes can show diverse sensitivities to even the same CE. Further, CEs, often initiated by large-scale atmospheric circulation and sea surface temperature anomalies (Kornhuber et al., 2019; Rousi et al., 2022), may also be driven by two or more climate drivers simultaneously. Research suggests that compound CEs are more likely to exacerbate but also could alleviate the impacts of individual ones on vegetation growth (Hoover et al., 2022; Zscheischler et al., 2020). Considering these complexities in CEs and the associated vegetation responses, it is of particular importance to attribute NEGs to different individual and compound CEs. Such improved understanding of NEGs and their association with various types of CEs is critical to project vegetation growth and subsequent carbon cycle feedbacks under future climate change, as well as to support ecosystem management under increasing climate change-driven risks (Anderegg et al., 2020; Reichstein et al., 2013).

The primary goals of this study are to detect NEGs during the past three decades and to investigate the extent to which multiple CE types drive these vegetation anomalies. Therefore, we perform a coincidence analysis between NEGs derived from satellite-derived normalized difference vegetation index (NDVI) and different types of CEs during the period 1981–2015 (see Section 2). Here we consider five individual CEs (i.e., atmospheric drought, soil drought, heatwave, frost, flood) and six compound CEs (Table S1). The robustness of our results is further tested with analysis of NEGs from global tree-ring width index (RWI) records from 2992 sites (predominantly in the Northern Hemisphere). We use the site-level standardized tree-ring chronologies since year 1982, in line with the satellite-based NDVI data. After determining any simultaneous coincidence between NEGs and CEs, we analyze the sensitivity of vegetation growth to different CEs to better understand the relative vulnerabilities underlying the association between NEGs and CEs.

2 | MATERIALS AND METHODS

2.1 | Data

2.1.1 | Satellite-based NDVI data

The NDVI is widely used to monitor the greenness and growth of vegetation. We use biweekly NDVI data from the third-generation Global Inventory Monitoring and Modelling System (GIMMS; Pinzon & Tucker, 2014). These data with an original spatial resolution of 1×1 km cover the period from 1982 to 2015. We aggregate NDVI data to a spatial resolution of $0.5\times0.5°$ to match the spatial resolution of the climatic data and removed pixels of unvegetated areas, defined by a mean annual NDVI <0.1.

2.1.2 | In-situ tree-ring data

We use the chronologies of tree-ring widths from the International Tree-Ring Data Bank (ITRDB) v7.15 (Grissino-Mayer & Fritts, 1997). The ITRDB provided site-level standardized chronologies from 2991 sites, mainly in the Northern Hemisphere. The raw data for the tree RWI are postprocessed by detrending, standardizing, and averaging

growth series of tree samples collected at the same site using the dplR package (v.1.6.8) in R. We use the site-level standardized chronologies since 1982, in line with the satellite-based NDVI data. Due to the limited number of sites with long records over the tropical and southern mid-latitudes, we only assess tree-ring chronologies from the north mid- and high-latitude regions (>25° N latitude).

2.1.3 | Climate data

Gridded data for monthly mean temperature, precipitation, and the number of frost days from 1982 to 2015 are obtained from the data set of the Climatic Research Unit (CRU v4.04; Harris et al., 2020) which has a spatial resolution of 0.5×0.5°. CRU climatic data are derived by the interpolation of monthly climatic anomalies with observations from extensive networks of meteorological stations (Harris et al., 2020). Gridded data for soil–water content are reanalyzed data from the European Centre for Medium Range Weather Forecasts Reanalysis 5 (ERA5; Hersbach et al., 2020). We use all data for four soil layers, 0–7, 7–28, 28–100, and 100–289 cm, and aggregated the data at a spatial resolution of 0.5×0.5° before further analysis. The monthly vapour-pressure deficit (VPD) is calculated as the difference between the actual and saturated vapour pressures, using data for temperature, specific humidity, and air pressure at a height of 2 m from the reanalyzed data set of Modern-Era Retrospective analysis for Research and Applications, Version 2 (MERRA-2; Gelaro et al., 2017).

2.2 | Analysis

2.2.1 | Identification of vegetation (NEGs) and CEs

We calculate the average biweekly NDVI of the growing season from 1982 to 2015. Information for the growing season is derived from Zhu et al. (2016). The long-term linear trend of growing-season NDVI is first detrended. Note the detrending procedure is used to avoid overestimation of variability due to potential trends that could have been driven by different factors such as elevated CO_2 concentration, nitrogen deposition, and long-term vegetation acclimation. The years of NDVI negative extremes (NEGs) are defined as years with NDVI anomalies below the 10th percentile of NDVI anomalies during 1982–2015. We also test different definitions of extreme events, for example, we use mean minus 1.5 SD as the threshold, where SD is the standard deviation of growing-season NDVI anomalies, and we verify that the attribution results are robust with respect to the definition of extremes (Figure S1). Site-level standardized RWI chronologies use the same 10th percentile to define RWI negative extremes and are, therefore, similar to our use of NDVI data. In this study, we only focus on the negative extreme anomalies in vegetation growth, which have serious damage to terrestrial ecosystems. Note that we exclude all the vegetation negative extremes in 1991 and 1992 to avoid the effects of the Pinatubo volcanic eruption because the aim of this analysis is to determine the impacts of climate on negative vegetation growth extremes.

We consider five types of CEs: cold extremes (Tmp−; also called frost), heatwaves (Tmp+), high VPD extremes (VPD+, also called atmospheric drought), soil drought (WA−), and positive extremes of water availability (WA+; also called flood). We use several climatic indexes to define CEs using the same percentile method applied to vegetation extremes. For Tmp−, the time series of average monthly temperature, minimum monthly temperature, and the number of frost days during the growing season are detrended. Anomalies of average temperature or minimum temperature below their 10th percentile, or anomalies of the number of frost days above their 90th percentile are defined as Tmp−. For Tmp+, the time series of average monthly temperature and maximum monthly temperature during the growing season are detrended. Anomalies of average temperature or maximum temperature above their 90th percentiles are defined as Tmp+. Similarly, the average monthly VPD and maximum monthly VPD during the growing season are used to define VPD+. Anomalies of the average VPD or maximum VPD above their 90th percentile are defined as VPD+. For WA− and WA+, we use average monthly precipitation and average soil-water content for four soil layers (0–7, 7–28, 28–100 and 100–289 cm). Anomalies of average precipitation or average soil-water content below their 10th percentiles were defined as WA− whereas anomalies of average precipitation or average soil-water content above their 90th percentiles were defined as WA+.

We also consider compound CEs, that is, two or more CEs occurred simultaneously. Six types of compound CEs are investigated in this study: Tmp−&WA−, Tmp−&WA+, Tmp+&WA−, Tmp+&WA+, VPD+&WA− and VPD+&Tmp+&WA− (Table S1). The other compound extremes are excluded from this study because they are associated with less than 1% of NEGs globally. In Figure 2c,d, Tmp is abbreviated as T, WA as W and VPD as V.

2.2.2 | Coincidence analysis for NEGs and CEs

We conduct a coincidence analysis (Rammig et al., 2015) that quantifies the coincidence between NEGs and each individual and compound CE. The rate of coincidence is an index that indicates how many NEGs coincide with CEs from all the vegetation extremes detected during 1982–2015 for all grids in each 15×15 spatial moving windows. For the global rates of coincidence in Figure 2a,c, we sum the coincidences between NEGs and CEs for all sites or 0.5° grid cells around the globe, and divide them by the number of all NEGs for the sites (RWI) or 0.5° grid cells (NDVI). The individual and compound CEs with the highest coincidences are selected separately and considered the dominant drivers of NEGs. For tree-ring data, according to the coordinate information of each site, we can identify the 0.5° grid cells where they are located. For each site, we take the grid cell in which the site is located, find all the other sites located in adjacent grid cells within a 15×15 spatial moving window, and then use these sites together to do the coincidence analysis.

Here, we test if the coincidence rate of each dominant CE is significantly higher than the coincidence rates of the CE when they occur randomly in a time series. We randomly shuffle the times series of the yearly data of all climate variables, but keep the time series of growing-season NDVI unaltered. Then, we use the same method to identify NEGs, and individual and compound CEs. Next, we calculate the coincidence rate of each CE with NEGs. We repeat the random shuffling 1000 times and calculate the coincidence rate of each CE with NEGs in random time series. Lastly, for all study regions, we compare the coincidence rate of the dominant CE estimated by our randomly shuffled climate time series with the coincidence rate calculated using the original unaltered climate time series. We find, for almost study regions, the coincidence rate of the dominant CE is significantly greater than that estimated by randomly shuffled climate time series, based on the Student's *t*-test ($p < .05$, Figure S2). Hence, this confirms the connection between CEs and NEGs cannot occur simply at random.

2.2.3 | Sensitivity of vegetation and frequency, intensity, and duration of CEs

The risk and impact of CE events in the Intergovernmental Panel on Climate Change (IPCC) report is characterized by 'hazard', 'exposure', and 'vulnerability' (Field et al., 2012). We use this framework to calculate the frequency of each individual or compound CE (representing 'hazard'), the intensity and duration of the CE (representing 'exposure'), and the sensitivity of vegetation to the CE (with NEG representing 'vulnerability'). Frequency is calculated as the probability of CE occurrence during 1982–2015 inclusive, for all grids in the a 15×15 spatial moving window. Intensity (or duration) is calculated as the mean intensity (or duration) of all extreme events during 1982–2015 for all grids in the 15×15 spatial moving windows. Sensitivity is calculated as the mean of vegetation anomalies during the years of CE divided by the mean of the intensity of CE. All years with negative vegetation anomalies (NDVI anomalies <0) in response to the CE are included. Years with positive vegetation anomalies are excluded because such positive responses are likely to be caused by other climatic factors or human management.

2.2.4 | Changes in the response of NDVI to individual and compound CEs

We conduct this analysis for regions where the dominant compound extreme is the combination of the dominant individual extreme and another CE. We compare the sensitivity of vegetation to compound CEs and that to every individual CE at the same intensity. For example, in one pixel in Amazon, the dominant individual CE is WA− and the dominant compound CE is WA−&VPD+. We compare the sensitivity of vegetation to the same intensity of WA− with and without VPD+. The detailed methods are as follows: First, we select all individual and compound CE events during 1982–2015 for all grids in each 15×15 spatial moving windows. Second, all individual and compound extremes are then sorted into 13 bins according to their intensity: 1.2–1.3, 1.3–1.4, ..., 2.3–2.4 and 2.4–2.5, where SD is from their historical climatic distributions. Third, we calculate the differences in the average NDVI anomalies (only if NDVI anomalies <0) between the occurrence of individual CEs and the occurrence of compound extremes for each intensity bin. Finally, we calculate the mean of the NDVI anomalies difference between individual and compound CEs across all intensity bins.

3 | RESULTS AND DISCUSSION

3.1 | The coincidence of individual and compound CEs with extreme reductions in vegetation growth

We define NEGs as continuous time periods when the current NDVI value is less than the 10th percentile of the historical NDVI distribution. Figure 1a illustrates the coincidence of NEGs with individual and compound CEs (which are similarly defined by the 10th or 90th percentiles of historical distributions; see Section 2) at the global scale. Our headline finding is that the coincidence between NEGs and CEs is relatively high in semi-arid and arid regions, as well as in northern mid-latitude regions such as northeastern China and India, eastern Europe, northeastern United States, and southern Canada. In the Southern Hemisphere, we find a high coincidence between NEGs and CEs in southern Africa and northern Australia. In these regions, almost 70% of the NEGs could be attributed to different types of CEs. The residues in this coincidence analysis may have been partly due to the limited reliability of the climatic data (Harris et al., 2020), or extensive direct human activities that affect vegetation growth (Davis et al., 2020). Furthermore, part of any remaining inconsistency between NEGs and CEs could also be explained by the lagged impacts of CEs (Anderegg et al., 2015), for example in the epicenter of the 2005 and 2015/16 Amazonian droughts (Saatchi et al., 2013; Yang et al., 2022). In addition, natural disturbances such as wildfire and windthrow, or other biotic disturbance agents such as insect pests and pathogens, which are not completely aligned with meteorological conditions, may also affect vegetation growth (Balzter et al., 2007; Forzieri et al., 2021; Hicke et al., 2012).

For the regions where NEGs have high coincidence with CEs, individual CEs contribute about 40%–50%, while the rest half are coincident with compound CEs (Figure 1b). By contrast, in the humid tropics, southeastern China, and part of Siberia, the coincidence between NEGs and compound CEs is relatively low. That is, in these regions, most NEGs are associated with individual CEs (colored red in Figure 1b). Even when we relax the definition for compound CE events as 20th and 80th percentiles, only about 3% of NEGs coincide with compound CEs in these regions (Figure S3). Furthermore, as an independent verification of our findings, NEGs derived from tree-RWI show similar patterns in their coincidence with CEs (bottom insets in Figure 1a,b), confirming the robustness of our results.

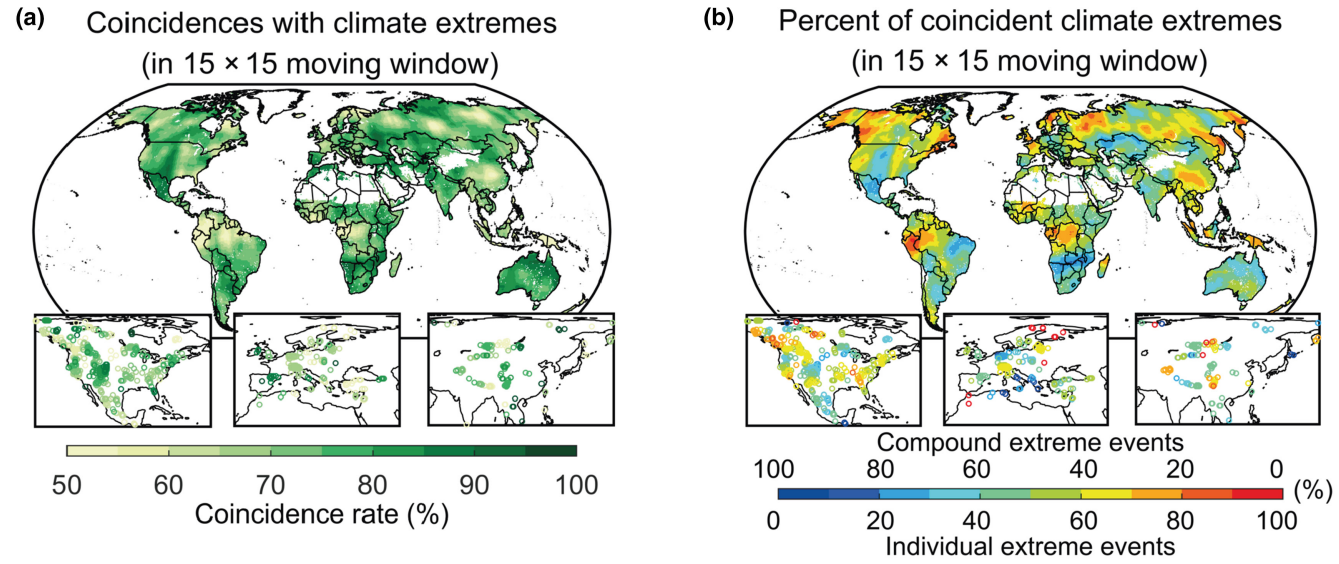

FIGURE 1 Coincidence of NDVI and RWI negative extremes with individual and compound climate extremes. (a) Total rates of coincidence of NDVI and RWI negative extremes with individual and compound climatic extremes. (b) Fraction of the total rate of coincidence for individual and compound climatic extremes. Reds donate a higher rate of coincidence for individual climatic extremes, while blues donate a higher coincidence rate for compound climate extremes. Map lines delineate study areas and do not necessarily depict accepted national boundaries. NDVI, normalized difference vegetation index; RWI, ring width index.

Next, we identify the dominant individual and compound CEs coincident with NEGs. For individual CEs, soil drought (defined by the 10th percentiles of precipitation and soil water content of four different soil layers, WA−) has the highest occurrence rate with NEGs (13% for NDVI, 12% for RWI, Figure 2a). These NEGs coincident with soil drought occur mainly in pan-tropic regions including tropical semi-arid regions (Figure 2b), where soil drought is the primary factor limiting vegetation growth (Li et al., 2021; Walther et al., 2019). It is particularly noteworthy that although the wet tropical region is in general not water-limited, massive vegetation declines like tree mortality are also widely observed in this area under extreme soil droughts (for example, Bonal et al., 2016; Corlett, 2016) which are induced by El Niño-Southern Oscillation (ENSO) or elevated surface temperatures of the Atlantic Ocean. However, some of these areas, including parts of the upper Amazon and Congolese Basins, also have negative vegetation growth anomalies under extreme wet conditions (Figure 2b), when pulse flooding may cause tree mortality (Resende et al., 2020). In northern mid- and high-latitude regions such as the basins of the Yangtze River in China, the Ob, Yenisey and Lena Rivers in Siberia, and the Yukon and Mackenzie Rivers in Canada, it is also wet extremes of soil water, usually associated with water inundation and flooding, that had the highest coincidence rate with NEGs (Figure 2b). In these regions, besides flood damages, the reduced radiation and low temperature, along with heavy precipitation events, may also add to the risk of widespread plant mortality and thus NEGs. Furthermore, in mountainous areas of North America, Europe, and northern Siberia, NEGs are mostly associated with cold extremes (Figure 2b).

Warming-induced increases in VPD have been suggested to play an increasingly important role in suppressing vegetation growth (Grossiord et al., 2020; Novick et al., 2016; Yuan et al., 2019). However, we rarely find extremely high VPD as the only factor accounting for NEGs (Figure 2a), which is likely related to the fact that high VPD extremes rarely occurred individually (Figure S4). Instead we do find compound CEs involving high VPD extremes, i.e., VPD+&WA− and VPD+&Tmp+&WA−, have high coincidences with NEGs (Figure 2c). Such VPD-associated compound events often involve a strong coupling of VPD and soil moisture, which can cause severe vegetation degradation (Seneviratne et al., 2010; Zhou et al., 2019). Geographically, these VPD-associated CEs (i.e., VPD+&WA− and VPD+&Tmp+&WA−) as dominant compound CEs are coincident with NEGs in tropical and temperate drylands (Figure 2d). At these locations, high VPD and soil water deficits together trigger major stomatal closure to minimize water loss, at the cost of strongly inhibited plant photosynthesis. The closure of stomata reduces evapotranspiration and thus evaporative cooling effect, leading to further local warming and a rise in VPD (Hauser et al., 2016; Zhang et al., 2020). This positive feedback can prompt additional reduction in photosynthesis. The other type of compound CE that has substantially high coincidence with NEGs is Tmp−&WA+, which mainly appears in boreal regions (>60° N) (Figure 2d).

3.2 | The underlying mechanisms linking extreme reductions in vegetation growth to CEs

Both the characteristics of CEs and the sensitivities of different ecosystems to CEs could contribute to the observed coincidence between CEs and NEGs (Frank et al., 2015). Hence, we further explore the underlying mechanisms that link NEGs to

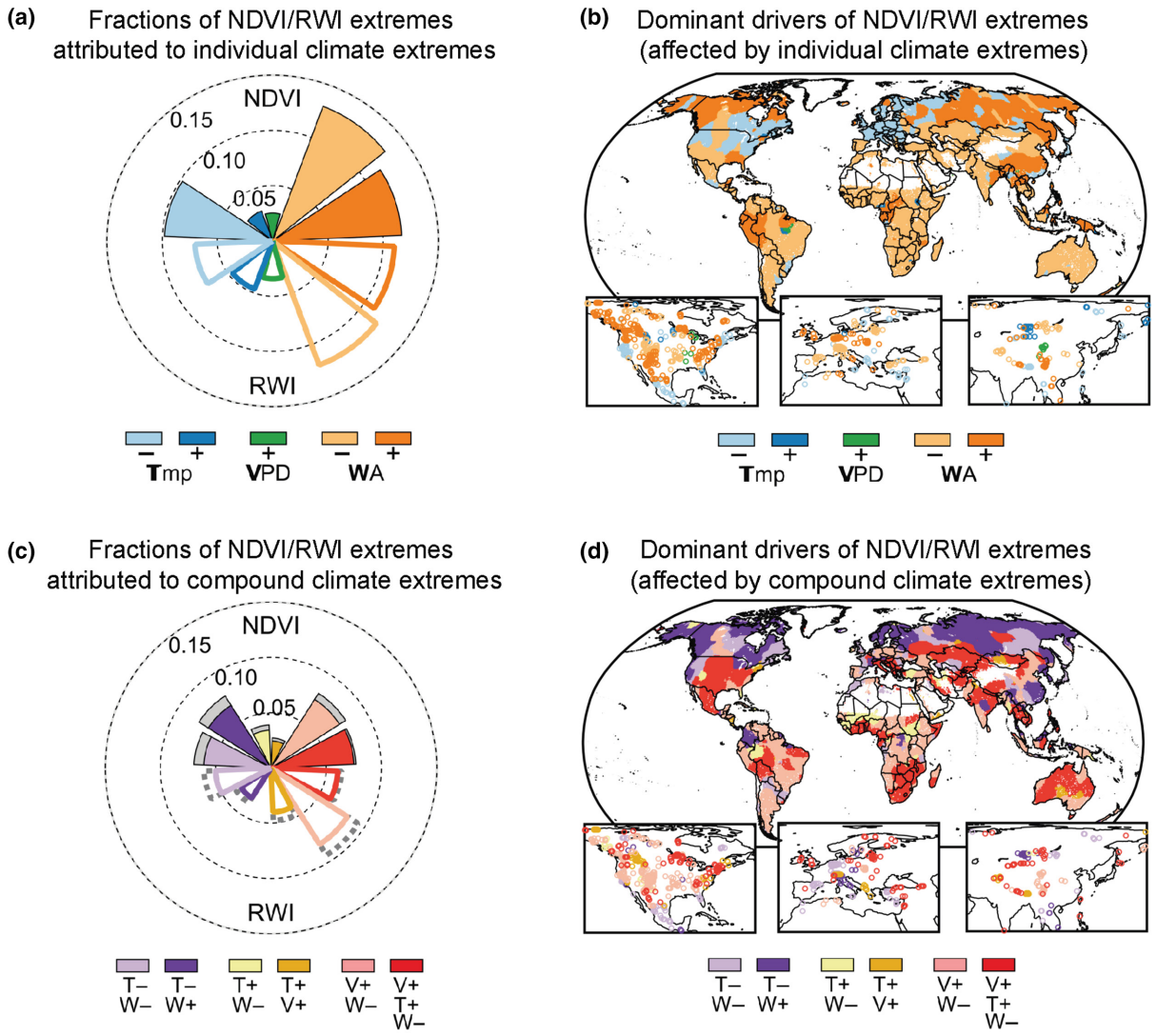

FIGURE 2 Fractions of NDVI and RWI negative extremes coincident with each individual and compound climate extreme. (a) Fractions of all NDVI or RWI negative extremes during 1982–2015 (excluding 1991 and 1992) coincident with five individual climatic extremes (Tmp−, Tmp+, VPD+, WA− and WA+) for all grids or sites around the globe. The filled and outlined areas are fractions of NDVI and RWI negative extremes, respectively. (b) Spatial pattern of dominant individual climatic extremes coincident with the most NDVI or RWI negative extremes. (c) Fractions of NDVI or RWI negative extremes coincident with six compound climatic extremes: Tmp−&WA−, Tmp−&WA+, Tmp+&WA−, Tmp+&WA+, VPD+&WA− and VPD+&Tmp+&WA−. The gray filled and outlined areas are the fractions of NDVI and RWI negative extremes coincident with moderate compound climatic extremes (defined by the 20th/80th percentiles). (d) Spatial pattern of dominant compound climatic extremes, including moderate compound extremes, coincident with the most NDVI or RWI negative extremes. Map lines delineate study areas and do not necessarily depict accepted national boundaries. NDVI, normalized difference vegetation index; RWI, ring width index.

their dominant CEs. Following an IPCC analysis framework for impacts, this mechanistic assessment focuses on the frequency of CEs, the exposure of vegetation to CEs (characterized by the intensity and duration of CEs), and the vulnerability of vegetation to CEs (see Section 2.2.3). First, for individual CEs, we find that the frequency of dominant individual CEs is higher than the occurrence of other individual CEs across most vegetated areas (90%; Figure 3a; Figure S4). Furthermore, we find that although exposure risks to CEs also contribute to the high coincidence with NEGs, the intensity and duration of individual CEs play regionally-divergent roles (Figure 3b; Figure S5). In wet tropics, NEGs that correspond to dominant individual CEs have both higher intensity and longer duration than other individual CEs (colored purple in Figure 3b). In the dry tropics, as well as some temperate regions such as Australia, South Africa, and parts of China, a longer duration is more important than higher intensity for individual CEs being dominant (colored orange in Figure 3b). In the mountainous areas of North America, Europe, and northern Siberia, only the intensity of the dominant individual CEs is higher than that of other individual CEs (colored red in Figure 3b). Second, unlike individual CEs, high frequency is often not a key feature determining the dominance of compound CEs (Figure 3c; Figure S6). However, in

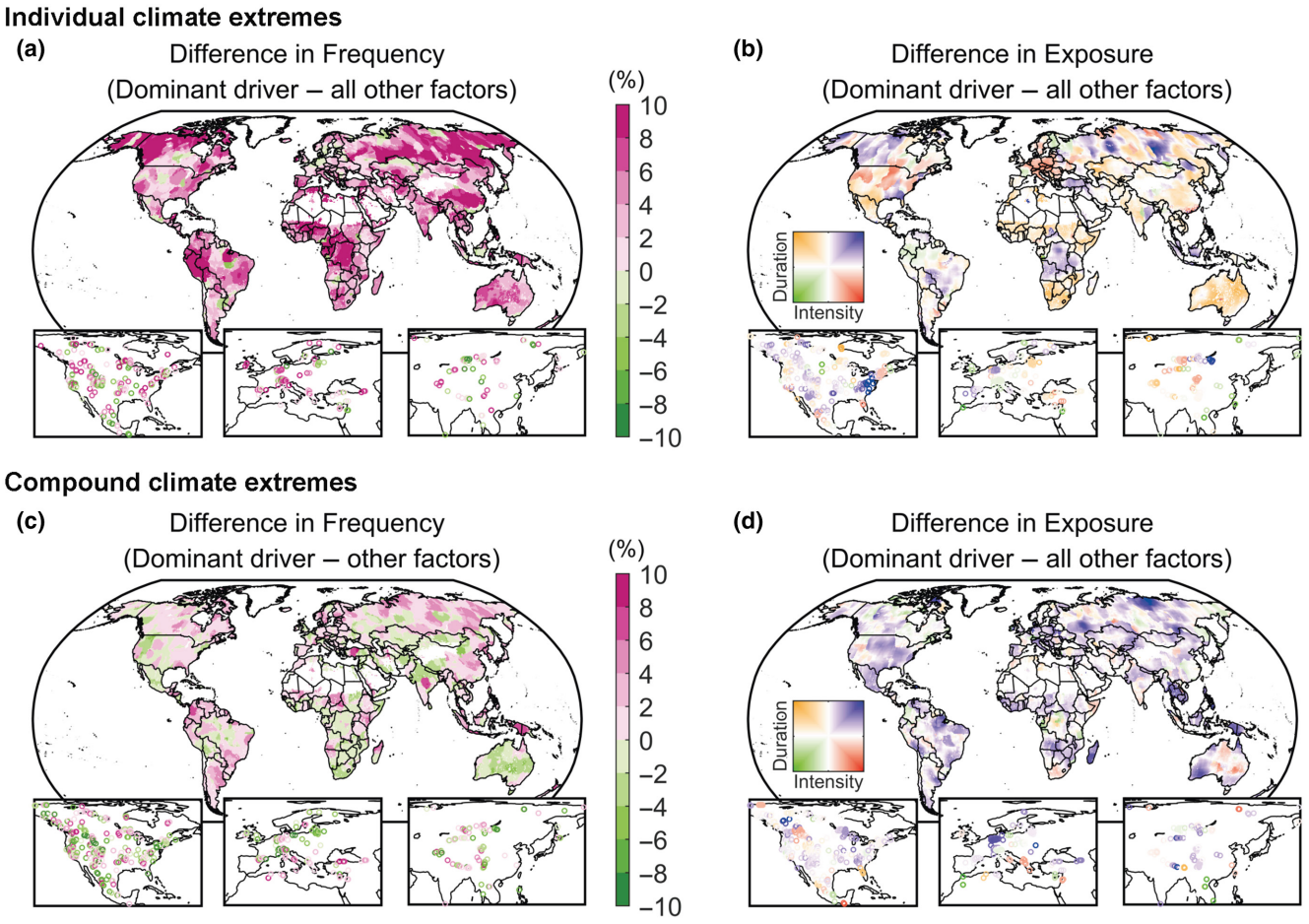

FIGURE 3 Comparison of frequency and exposure among different climate extremes. (a, b) Differences in frequency (a) and exposure (reflected by intensity and duration) (b) of the dominant individual climate extreme and other individual climatic extremes. (c, d) The same results as (a, b) but for compound climatic extremes. Map lines delineate study areas and do not necessarily depict accepted national boundaries.

almost all vegetated areas, both the intensity and duration of the dominant compound CEs are higher than those of other compound CEs (Figure 3d; Figure S7).

The vulnerability of vegetation to CEs also plays an important role in the high coincidence between NEGs and individual CEs. Figure 4a illustrates that, with similarities to the impacts of frequency, the sensitivity (as a metric reflecting vulnerability) of vegetation to dominant individual CEs is higher than that to the other individual CEs over almost all the global vegetated area (91%). This is in accordance with the general ecological theory that unstable ecosystems likely have an amplified response to perturbations, such as CEs (Scheffer et al., 2009; Seddon et al., 2016). In all cases, we find that climatological conditions and forest cover fractions determine the spatial distributions of sensitivity of vegetation to CEs (Figure 5). More specifically, the sensitivity of vegetation to negative extremes of soil water availability (WA−) increases, as expected, with decreasing soil moisture but also with reduced forest cover fraction. Alternatively, the sensitivity of vegetation to extreme atmospheric drought (VPD+) actually increases with forest cover fraction. Therefore, low tree-cover regions have high sensitivities to soil water drought, for example, in dry tropics and temperate arid/semi-arid regions, while high tree-cover regions have high sensitivity to atmospheric water drought (Figure 5c,d). This divergence may be due to distinct plant growth and water-use strategies. In regions with high forest coverage, plants tend to adopt a fast-growing productive strategy to outcompete their neighbors for resources (Forrester, 2019). As a cost of this strategy, these plants could be more vulnerable to resource scarcity when high VPD forces the reduction in stomatal conductance. In dry ecosystems where tree cover is usually low, plants often adopt a conservative growth strategy to reduce water loss from stomatal conductance. For these ecosystems, severe soil water depletion poses a greater threat to plant growth and survival, and subsequently the stability of ecosystems (Hoover et al., 2014; Liu et al., 2020). Unlike soil and atmospheric water drought, the sensitivity of vegetation to cold extremes (Tmp−) increases with increasing forest cover fraction and decreasing temperature. The sensitivity to Tmp− is pronounced in the dense forests or shrublands at the high northern latitudes (Figure S8). In these regions, temperature, which co-varies with energy (radiation), is the primary limiting factor for vegetation growth.

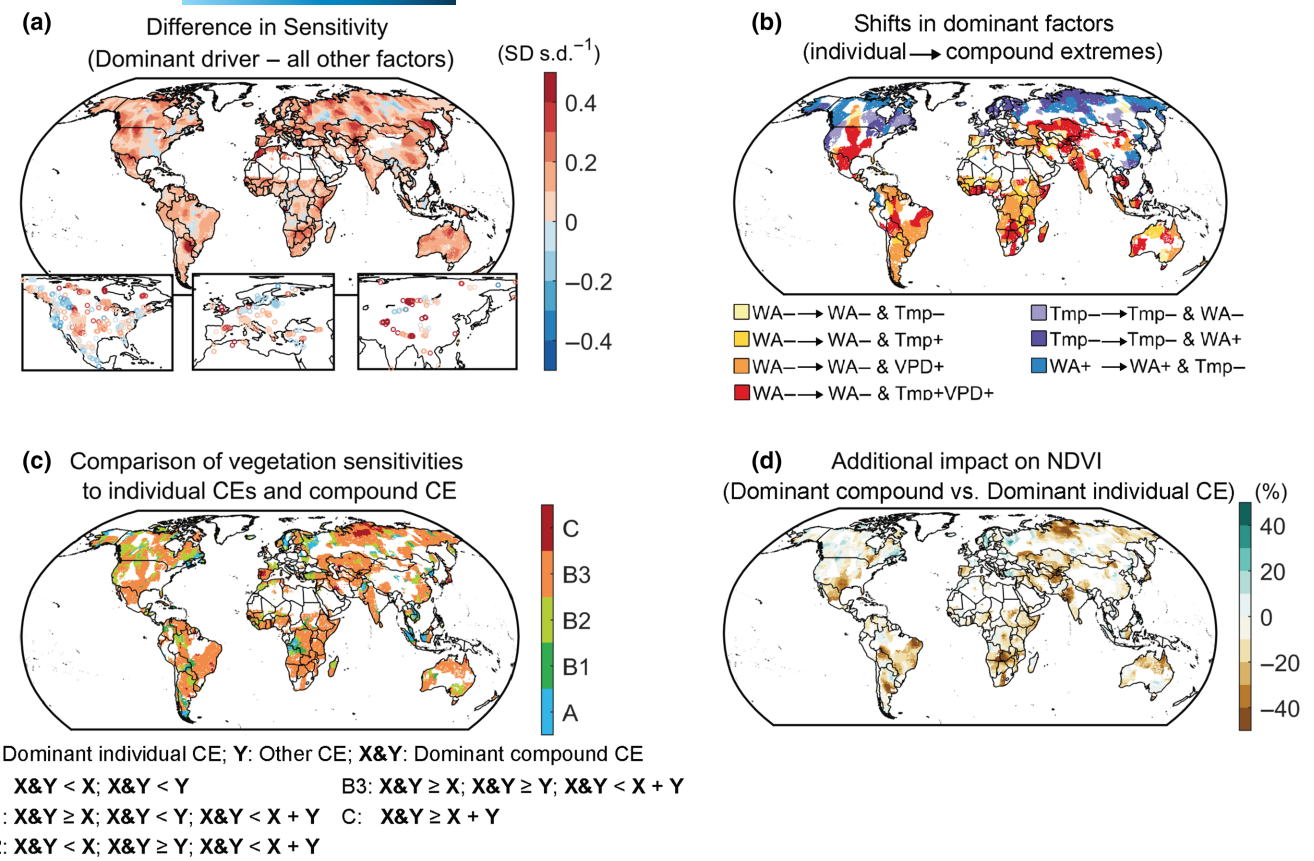

FIGURE 4 Comparison for the vulnerability of vegetation to different CEs. (a) Differences of the vulnerability of vegetation to dominant individual CE and that to other individual CEs. (b) Comparison of the dominant individual CE and the dominant compound CE. Only regions where the dominant compound CE is a combination of the dominant individual CE and another CE are shown. (c) Comparison of sensitivities of NDVI to dominant compound CE and every individual CE. There are five relationships: A, B1, B2, B3 and C. Relationship A (colored blue) represents less sensitivity to compound CE than to all individual CEs; Relationship B (B1–B3, colored greens) represents higher sensitivity to compound CE than at least one individual CE; Relationship C (colored red) represents sensitivity to compound CE greater than the sum of sensitivity to all individual CEs. (d) Difference in sensitivities of NDVI to dominant compound CE and dominant individual CE. Map lines delineate study areas and do not necessarily depict accepted national boundaries. CE, climate extreme; NDVI, normalized difference vegetation index.

More complex environmental conditions, for example, co-occurrence of multiple CEs, has been observed to become frequent and severe under climate change (AghaKouchak et al., 2014). Yet, a knowledge gap exists in whether vegetation will become more vulnerable to two or three concurrent CEs (as investigated here). According to Liebig's "law of the minimum", vegetation growth rate is primarily determined by the most limiting factor (Sinclair, 1994). Application of Liebig's law of the minimum, however, does not always consider the interactions among multiple factors that can have additive or antagonistic effects. That is, as we illustrate, compound CEs can exacerbate or alleviate the impacts of individual CEs on vegetation. Our results suggest that for most regions, vegetation shows a higher sensitivity to compound CEs than to every individual CE of the same intensity, but lower than the sum of sensitivities to individual CEs (colored orange in Figure 4c). On average, our identified compound CEs cause an additional reduction of 11% in NDVI than the averaged impact of individual CEs (Figure 4b,d). In particular, when three CEs occur simultaneously, i.e., VPD+&Tmp+&WA−, they can cause a reduction of 23% in NDVI on average. Soil water deficits reduce water supply to plants whereas high VPD (usually associated with high temperature) enhances atmospheric demand for water and increases plant water loss (Seneviratne et al., 2010). Their compound effects, therefore, result in greater water limitation on plant photosynthesis and growth compared to individual impacts. We do, however, find a few regions where the vegetation sensitivity to compound CEs is nearly equal to its sensitivity to one individual CE (colored greens in Figure 4c), conforming more closely to Liebig's law of the minimum. For example, vegetation shows similar sensitivities to compound CEs of Tmp−&WA+ and to individual CEs of Tmp−. Cold extremes (Tmp−) could lead to delayed growing season and suppress vegetation growth in temperate and boreal regions (Zohner et al., 2020), reducing the vegetation demands for water and nutrients. As a result, vegetation might be less sensitive to the lack of resources imposed by other stresses. Although we use the sensitivity of decline in NDVI to simultaneous CEs to assess the vulnerability of vegetation, other metrics such as vegetation recovery time and rate after different types of CEs are likely also important

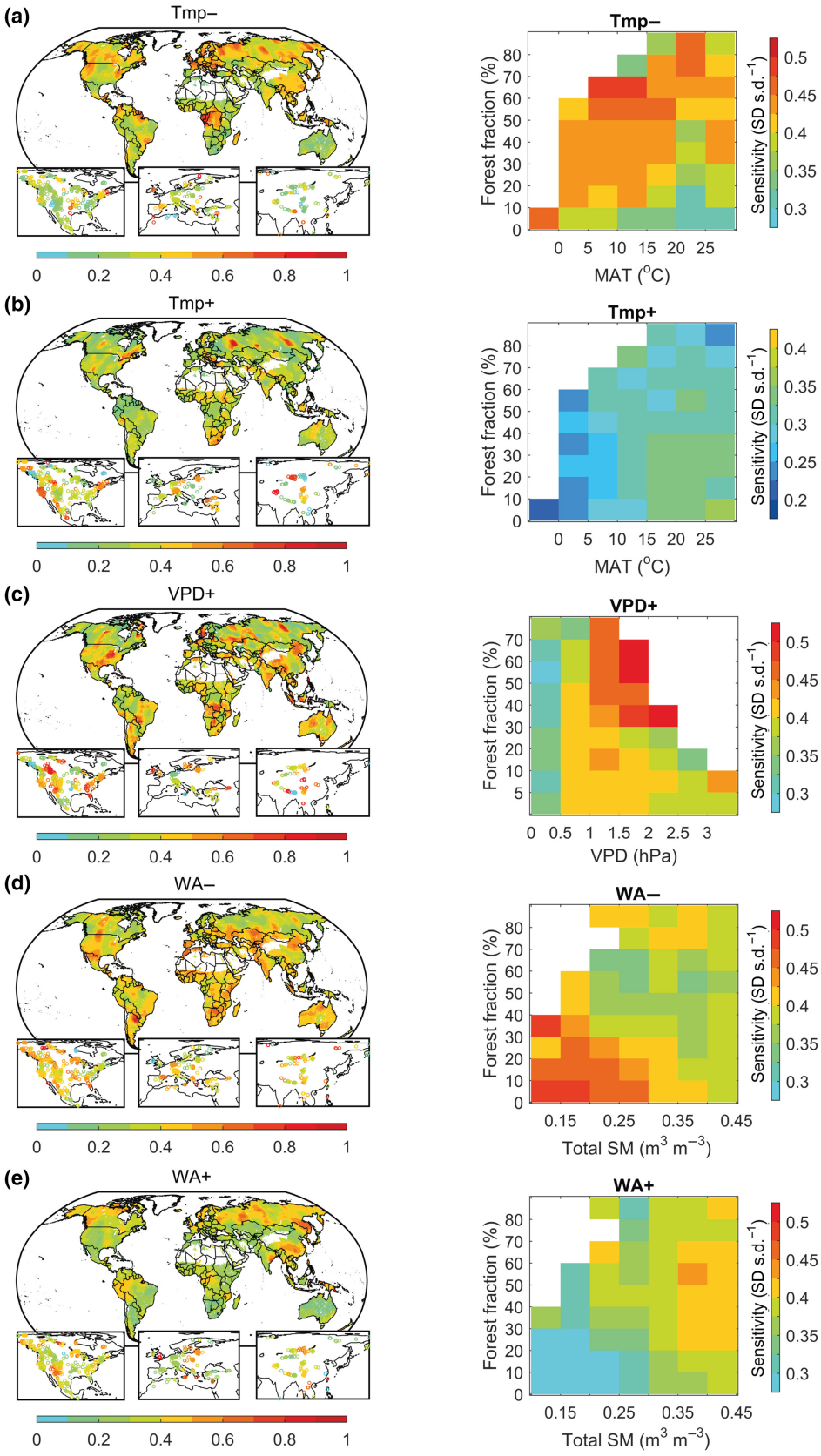

FIGURE 5 The sensitivity of NDVI and RWI to five individual climate extremes. (a) Tmp−, (b) Tmp+, (c) VPD+, (d) WA− and (e) WA+. The right-hand panels show the sensitivity of NDVI and RWI to individual climate extreme across climate and vegetation regimes. Map lines delineate study areas and do not necessarily depict accepted national boundaries. NDVI, normalized difference vegetation index; RWI, ring width index.

for overall vulnerability assessment and need to be investigated in future studies.

4 | SUMMARY AND IMPLICATIONS

An improved understanding of the CEs responsible for major suppression of vegetation growth is important. Such knowledge provides more reliable projections of risks to vegetation, and can inform adaptation strategies, under on-going climate change. We identify widespread instances of negative extremes in vegetation growth (NEGs) over the last three decades. Further, we link these negative vegetation growth responses to different individual and compound CEs. Specifically, droughts and drought-related compound extremes (with high VPD and/or heatwave) are primarily responsible for most NEGs observed in the wet tropics, arid and semi-arid regions. NEGs in mountainous regions of North America, Europe, and northern Siberia are often associated with cold extremes, hydrological wet extremes, or their compound occurrence. Furthermore, in most regions, compound CEs could generally lead to more negative impacts than individual extremes on vegetation growth. Thus, improving our understanding of, and capacity to predict, compound CEs and their impacts on ecosystems remains a research priority.

Compelling evidence suggests that the simultaneous occurrence of different types of CEs, i.e., the risk of compound CEs, is also likely to increase in both frequency and intensity under future climate change (Fischer et al., 2021; IPCC, 2021). For example, concurrent extremes of soil droughts and heatwaves, or of soil droughts and atmospheric droughts, are projected to become more frequent and intense because of land-atmosphere feedbacks (Hauser et al., 2016; Sarhadi et al., 2018). More frequent, intense, and longer CEs, assuming no substantial changes in vegetation sensitivity, are likely to induce more substantial reductions in vegetation growth. Furthermore, seasonal and sub-seasonal CEs such as flash droughts (Otkin et al., 2019; Pendergrass et al., 2020) and heatwaves (Lin et al., 2022) could also have large impacts on vegetation growth due to their more rapid development and potential raised severity. Extending future analyses to these finer time scales may help gain additional insight into detecting and attributing NEGs. Moreover, enhanced vegetation sensitivities over almost all the global vegetated areas may amplify these reductions further, leading to more widespread vegetation losses. The future risk of NEGs, however, could be partly offset by the physiological effects of elevated atmospheric CO_2 and by vegetation acclimation and species turnover (Keenan et al., 2013; Peters et al., 2018). Therefore, further research is required to determine the effects of any evolving ecosystem resistance and resilience as atmospheric greenhouse gases rise. This overall area of research into combined CEs and vegetation response is essential for guiding effective policy and mitigative strategies.

ACKNOWLEDGEMENTS

This study was supported by the National Natural Science Foundation of China (grant number 41988101), the U.S. Department of Energy (grant number DE-SC0022074), and the German Federal Ministry of Economics and Technology (grant number 50EE1904). S.M.M. was supported by the USGS Ecosystems Mission Area. C.H. was supported by the NERC National Capability award to UKCEH. J.P. was supported by the grant TED2021-132627B-I00 funded by MCIN, AEI/10.13039/501100011033 and by the European Union NextGenerationEU/PRTR. Any use of trade, product, or firm names in this paper is for descriptive purposes only and does not imply endorsement by the U.S. Government.

CONFLICT OF INTEREST

The authors declare that they have no conflict of interest.

DATA AVAILABILITY STATEMENT

All data needed to evaluate the conclusions in the paper are present in Section 2 and/or the Supplemental Information. GIMMS 3g NDVI are downloaded from: https://climatedataguide.ucar.edu/climate-data/ndvi-normalized-difference-vegetation-index-3rd-generation-nasagfsc-gimms (doi: 10.3390/rs6086929); Tree ring data are downloaded from: https://www1.ncdc.noaa.gov/pub/data/paleo/treering/; CRU climate data are downloaded from: https://crudata.uea.ac.uk/cru/data/hrg/ (doi: https://doi.org/10.1038/s41597-020-0453-3); ERA5 soil moisture data are downloaded from: https://cds.climate.copernicus.eu/cdsapp#!/dataset/reanalysis-era5-single-levels-monthly-means?tab=overview (doi: 10.24381/cds.f17050d7).

ORCID

Seth M. Munson https://orcid.org/0000-0002-2736-6374
Chris Huntingford https://orcid.org/0000-0002-5941-7770
Nuno Carvalhais https://orcid.org/0000-0003-0465-1436
Alan K. Knapp https://orcid.org/0000-0003-1695-4696
Josep Peñuelas https://orcid.org/0000-0002-7215-0150
Anping Chen https://orcid.org/0000-0003-2085-3863

REFERENCES

AghaKouchak, A., Cheng, L., Mazdiyasni, O., & Farahmand, A. (2014). Global warming and changes in risk of concurrent climate extremes: Insights from the 2014 California drought. *Geophysical Research Letters*, *41*(24), 8847–8852.

Anderegg, W. R., Schwalm, C., Biondi, F., Camarero, J. J., Koch, G., Litvak, M., Ogle, K., Shaw, J. D., Shevliakova, E., Williams, A. P., Wolf, A., Ziaco, E., & Pacala, S. (2015). Pervasive drought legacies in forest ecosystems and their implications for carbon cycle models. *Science*, *349*(6247), 528–532.

Anderegg, W. R., Trugman, A. T., Badgley, G., Anderson, C. M., Bartuska, A., Ciais, P., Cullenward, D., Field, C. B., Freeman, J., Goetz, S. J., Hicke, J. A., Huntzinger, D., Jackson, R. B., Nickerson, J., Pacala, S., & Randerson, J. T. (2020). Climate-driven risks to the climate mitigation potential of forests. *Science*, *368*(6497), eaaz7005.

Balzter, H., Gerard, F., George, C., Weedon, G., Grey, W., Combal, B., Bartholomé, E., Ergey Bartalev, S., & Los, S. (2007). Coupling of vegetation growing season anomalies and fire activity with hemispheric and regional-scale climate patterns in central and east Siberia. *Journal of Climate*, *20*(15), 3713–3729.

Bonal, D., Burban, B., Stahl, C., Wagner, F., & Hérault, B. (2016). The response of tropical rainforests to drought—Lessons from recent research and future prospects. *Annals of Forest Science*, *73*(1), 27–44.

Corlett, R. T. (2016). The impacts of droughts in tropical forests. *Trends in Plant Science*, *21*(7), 584–593.

Davis, K. F., Koo, H. I., Dell'Angelo, J., D'Odorico, P., Estes, L., Kehoe, L. J., Kharratzadeh, M., Kuemmerle, T., Machava, D., de Jesus Rodrigues Pais, A., Ribeiro, N., Rulli, M. C., & Tatlhego, M. (2020). Tropical forest loss enhanced by large-scale land acquisitions. *Nature Geoscience*, *13*(7), 482–488.

Felton, A. J. (2021). Response of terrestrial net primary productivity to precipitation extremes: Patterns, mechanisms, and uncertainties. In A. Fares (Ed.), *Climate change and extreme events* (pp. 57–81). Elsevier. https://doi.org/10.1016/B978-0-12-822700-8.09991-1

Field, C. B., Barros, V., & Stocker, T. F. (2012). *Managing the risks of extreme events and disasters to advance climate change adaptation*. Special report of the Intergovernmental Panel on Climate Change (IPCC). Intergovernmental Panel on Climate Change, Geneva (Switzerland). Cambridge University Press.

Fischer, E. M., Sippel, S., & Knutti, R. (2021). Increasing probability of record-shattering climate extremes. *Nature Climate Change*, *11*, 689–695. https://doi.org/10.1038/s41558-021-01092-9

Forrester, D. I. (2019). Linking forest growth with stand structure: Tree size inequality, tree growth or resource partitioning and the asymmetry of competition. *Forest Ecology and Management*, *447*, 139–157.

Forzieri, G., Girardello, M., Ceccherini, G., Spinoni, J., Feyen, L., Hartmann, H., Beck, P. S. A., Camps-Valls, G., Chirici, G., Mauri, A., & Cescatti, A. (2021). Emergent vulnerability to climate-driven disturbances in European forests. *Nature Communications*, *12*(1), 1–12.

Frank, D., Reichstein, M., Bahn, M., Thonicke, K., Frank, D., Mahecha, M. D., Smith, P., van der Velde, M., Vicca, S., Babst, F., Beer, C., Buchmann, N., Canadell, J. G., Ciais, P., Cramer, W., Ibrom, A., Miglietta, F., Poulter, B., Rammig, A., … Beer, C. (2015). Effects of climate extremes on the terrestrial carbon cycle: Concepts, processes and potential future impacts. *Global Change Biology*, *21*(8), 2861–2880.

Gampe, D., Zscheischler, J., Reichstein, M., O'Sullivan, M., Smith, W. K., Sitch, S., & Buermann, W. (2021). Increasing impact of warm droughts on northern ecosystem productivity over recent decades. *Nature Climate Change*, *11*(9), 772–779.

Gelaro, R., McCarty, W., Suárez, M. J., Todling, R., Molod, A., Takacs, L., Randles, C., Darmenov, A., Bosilovich, M. G., Reichle, R., Wargan, K., Coy, L., Cullather, R., Draper, C., Akella, S., Buchard, V., Conaty, A., da Silva, A., Gu, W., … Wargan, K. (2017). The modern-era retrospective analysis for research and applications, version 2 (MERRA-2). *Journal of Climate*, *30*(14), 5419–5454.

Grissino-Mayer, H. D., & Fritts, H. C. (1997). The International Tree-Ring Data Bank: an enhanced global database serving the global scientific community. *The Holocene*, *7*(2), 235–238.

Grossiord, C., Buckley, T. N., Cernusak, L. A., Novick, K. A., Poulter, B., Siegwolf, R. T., Sperry, J. S., & McDowell, N. G. (2020). Plant responses to rising vapor pressure deficit. *New Phytologist*, *226*(6), 1550–1566.

Harris, I., Osborn, T. J., Jones, P., & Lister, D. (2020). Version 4 of the CRU TS monthly high-resolution gridded multivariate climate dataset. *Scientific Data*, *7*(1), 1–18.

Hartmann, H., Moura, C. F., Anderegg, W. R., Ruehr, N. K., Salmon, Y., Allen, C. D., Arndt, S. K., Breshears, D. D., Davi, H., Galbraith, D., Ruthrof, K. X., Wunder, J., Adams, H. D., Bloemen, J., Cailleret, M., Cobb, R., Gessler, A., Grams, T. E. E., Jansen, S., … O'Brien, M. (2018). Research frontiers for improving our understanding of drought-induced tree and forest mortality. *New Phytologist*, *218*(1), 15–28.

Hauser, M., Orth, R., & Seneviratne, S. I. (2016). Role of soil moisture versus recent climate change for the 2010 heat wave in western Russia. *Geophysical Research Letters*, *43*(6), 2819–2826.

Hersbach, H., Bell, B., Berrisford, P., Hirahara, S., Horányi, A., Muñoz-Sabater, J., Nicolas, J., Peubey, C., Radu, R., Schepers, D., Simmons, A., Soci, C., Abdalla, S., Abellan, X., Balsamo, G., Bechtold, P., Biavati, G., Bidlot, J., Bonavita, M., … Thépaut, J.-N. (2020). The ERA5 global reanalysis. *Quarterly Journal of the Royal Meteorological Society*, *146*(730), 1999–2049.

Hicke, J. A., Allen, C. D., Desai, A. R., Dietze, M. C., Hall, R. J., Hogg, E. H., Kashian, D. M., Moore, D., Raffa, K. F., Sturrock, R. N., & Vogelmann, J. (2012). Effects of biotic disturbances on forest carbon cycling in the United States and Canada. *Global Change Biology*, *18*(1), 7–34.

Hoover, D. L., Hajek, O. L., Smith, M. D., Wilkins, K., Slette, I. J., & Knapp, A. K. (2022). Compound hydroclimatic extremes in a semi-arid grassland: Drought, deluge, and the carbon cycle. *Global Change Biology*, *28*(8), 2611–2621.

Hoover, D. L., Knapp, A. K., & Smith, M. D. (2014). Resistance and resilience of a grassland ecosystem to climate extremes. *Ecology*, *95*(9), 2646–2656.

IPCC. (2021). Summary for policymakers. In V. Masson-Delmotte, P. Zhai, A. Pirani, S. L. Connors, C. Péan, S. Berger, N. Caud, Y. Chen, L. Goldfarb, M. I. Gomis, M. Huang, K. Leitzell, E. Lonnoy, J. B. R. Matthews, T. K. Maycock, T. Waterfield, O. Yelekçi, R. Yu, & B. Zhou (Eds.), *Climate change 2021: The physical science basis. Contribution of Working Group I to the Sixth Assessment Report of the Intergovernmental Panel on Climate Change* (pp. 1514–1765). Cambridge University Press.

Keenan, T. F., Hollinger, D. Y., Bohrer, G., Dragoni, D., Munger, J. W., Schmid, H. P., & Richardson, A. D. (2013). Increase in forest water-use efficiency as atmospheric carbon dioxide concentrations rise. *Nature*, *499*(7458), 324–327.

Kornhuber, K., Osprey, S., Coumou, D., Petri, S., Petoukhov, V., Rahmstorf, S., & Gray, L. (2019). Extreme weather events in early summer 2018 connected by a recurrent hemispheric wave-7 pattern. *Environmental Research Letters*, *14*, 054002.

Lesk, C., Rowhani, P., & Ramankutty, N. (2016). Influence of extreme weather disasters on global crop production. *Nature*, *529*(7584), 84–87.

Li, W., Migliavacca, M., Forkel, M., Walther, S., Reichstein, M., & Orth, R. (2021). Revisiting global vegetation controls using multi-layer soil moisture. *Geophysical Research Letters*, *48*(11), e2021GL092856.

Lin, H., Mo, R., & Vitart, F. (2022). The 2021 western North American heatwave and its subseasonal predictions. *Geophysical Research Letters*, *49*(6), e2021GL097036.

Liu, L., Gudmundsson, L., Hauser, M., Qin, D., Li, S., & Seneviratne, S. I. (2020). Soil moisture dominates dryness stress on ecosystem production globally. *Nature Communications*, *11*(1), 1–9.

McDowell, N. G., Allen, C. D., Anderson-Teixeira, K., Aukema, B. H., Bond-Lamberty, B., Chini, L., Clark, J. S., Dietze, M., Grossiord, C., Hanbury-Brown, A., Hurtt, G. C., Jackson, R. B., Johnson, D. J., Kueppers, L., Lichstein, J. W., Ogle, K., Poulter, B., Pugh, T. A. M., Seidl, R., … Xu, C. (2020). Pervasive shifts in forest dynamics in a changing world. *Science*, *368*(6494), eaaz9463.

Novick, K. A., Ficklin, D. L., Stoy, P. C., Williams, C. A., Bohrer, G., Oishi, A. C., Papuga, S. A., Blanken, P. D., Noormets, A., Sulman, B. N., Scott, R. L., Wang, L., & Phillips, R. P. (2016). The increasing importance of atmospheric demand for ecosystem water and carbon fluxes. *Nature Climate Change*, *6*(11), 1023–1027.

Otkin, J. A., Zhong, Y., Hunt, E. D., Basara, J., Svoboda, M., Anderson, M. C., & Hain, C. (2019). Assessing the evolution of soil moisture and vegetation conditions during a flash drought–flash recovery sequence over the South-Central United States. *Journal of Hydrometeorology*, *20*(3), 549–562.

Overland, J. E., & Wang, M. (2021). The 2020 Siberian heat wave. *International Journal of Climatology*, *41*, E2341–E2346.

Pappas, C., Mahecha, M. D., Frank, D. C., Babst, F., & Koutsoyiannis, D. (2017). Ecosystem functioning is enveloped by hydrometeorological variability. *Nature Ecology & Evolution*, *1*(9), 1263–1270.

Pendergrass, A. G., Meehl, G. A., Pulwarty, R., Hobbins, M., Hoell, A., AghaKouchak, A., Bonfils, C. J. W., Gallant, A. J. E., Hoerling, M.,

Hoffmann, D., Kaatz, L., Lehner, F., Llewellyn, D., Mote, P., Neale, R. B., Overpeck, J. T., Sheffield, A., Stahl, K., Svoboda, M., … Woodhouse, C. A. (2020). Flash droughts present a new challenge for subseasonal-to-seasonal prediction. *Nature Climate Change*, *10*(3), 191–199.

Peters, W., van der Velde, I. R., Van Schaik, E., Miller, J. B., Ciais, P., Duarte, H. F., van der Laan-Luijkx, I. T., van der Molen, M. K., Scholze, M., Schaefer, K., Vidale, P. L., Verhoef, A., Wårlind, D., Zhu, D., Tans, P. P., Vaughn, B., & White, J. W. (2018). Increased water-use efficiency and reduced CO_2 uptake by plants during droughts at a continental scale. *Nature Geoscience*, *11*(10), 744–748.

Piao, S., Zhang, X., Chen, A., Liu, Q., Lian, X., Wang, X., Peng, S., & Wu, X. (2019). The impacts of climate extremes on the terrestrial carbon cycle: A review. *Science China Earth Sciences*, *62*(10), 1551–1563.

Pinzon, J. E., & Tucker, C. J. (2014). A non-stationary 1981–2012 AVHRR NDVI3g time series. *Remote Sensing*, *6*(8), 6929–6960.

Rammig, A., Wiedermann, M., Donges, J. F., Babst, F., Von Bloh, W., Frank, D., Thonicke, K., & Mahecha, M. D. (2015). Coincidences of climate extremes and anomalous vegetation responses: comparing tree ring patterns to simulated productivity. *Biogeosciences*, *12*(2), 373–385.

Reichstein, M., Bahn, M., Ciais, P., Frank, D., Mahecha, M. D., Seneviratne, S. I., Zscheischler, J., Beer, C., Buchmann, N., Frank, D. C., Papale, D., Rammig, A., Smith, P., Thonicke, K., van der Velde, M., Vicca, S., Walz, A., & Papale, D. (2013). Climate extremes and the carbon cycle. *Nature*, *500*(7462), 287–295.

Resende, A. F., Piedade, M. T., Feitosa, Y. O., Andrade, V. H. F., Trumbore, S. E., Durgante, F. M., Macedo, M. O., & Schöngart, J. (2020). Flood-pulse disturbances as a threat for long-living Amazonian trees. *New Phytologist*, *227*(6), 1790–1803.

Rousi, E., Kornhuber, K., Beobide-Arsuaga, G., Luo, F., & Coumou, D. (2022). Accelerated western European heatwave trends linked to more-persistent double jets over Eurasia. *Nature Communications*, *13*, 3851.

Saatchi, S., Asefi-Najafabady, S., Malhi, Y., Aragão, L. E., Anderson, L. O., Myneni, R. B., & Nemani, R. (2013). Persistent effects of a severe drought on Amazonian forest canopy. *Proceedings of the National Academy of Sciences of the United States of America*, *110*(2), 565–570.

Sarhadi, A., Ausín, M. C., Wiper, M. P., Touma, D., & Diffenbaugh, N. S. (2018). Multidimensional risk in a nonstationary climate: Joint probability of increasingly severe warm and dry conditions. *Science Advances*, *4*(11), eaau3487.

Scheffer, M., Bascompte, J., Brock, W. A., Brovkin, V., Carpenter, S. R., Dakos, V., Held, H., van Nes, E. H., Rietkerk, M., & Sugihara, G. (2009). Early-warning signals for critical transitions. *Nature*, *461*(7260), 53–59.

Seddon, A. W., Macias-Fauria, M., Long, P. R., Benz, D., & Willis, K. J. (2016). Sensitivity of global terrestrial ecosystems to climate variability. *Nature*, *531*(7593), 229–232.

Seneviratne, S. I., Corti, T., Davin, E. L., Hirschi, M., Jaeger, E. B., Lehner, I., Orlowsky, B., & Teuling, A. J. (2010). Investigating soil moisture–climate interactions in a changing climate: A review. *Earth-Science Reviews*, *99*(3–4), 125–161.

Sinclair, T. R. (1994). Limits to crop yield? In K. J. Boote, J. M. Bennett, T. R. Sinclair, & G. M. Paulsen (Eds.), *Physiology and determination of crop yield* (pp. 509–532). John Wiley & Sons, Ltd.

Walther, S., Duveiller, G., Jung, M., Guanter, L., Cescatti, A., & Camps-Valls, G. (2019). Satellite observations of the contrasting response of trees and grasses to variations in water availability. *Geophysical Research Letters*, *46*(3), 1429–1440.

Yang, H., Ciais, P., Wigneron, J. P., Chave, J., Cartus, O., Chen, X., Fan, L., Green, J. K., Huang, Y., Joetzjer, E., Kay, H., Makowski, D., Maignan, F., Santoro, M., Tao, S., Liu, L., & Yao, Y. (2022). Climatic and biotic factors influencing regional declines and recovery of tropical forest biomass from the 2015/16 El Niño. *Proceedings of the National Academy of Sciences of the United States of America*, *119*(26), e2101388119.

Yuan, W., Zheng, Y., Piao, S., Ciais, P., Lombardozzi, D., Wang, Y., Ryu, Y., Chen, G., Dong, W., Hu, Z., Jain, A. K., Jiang, C., Kato, E., Li, S., Lienert, S., Liu, S., Nabel, J. E. M. S., Qin, Z., Quine, T., … Yang, S. (2019). Increased atmospheric vapor pressure deficit reduces global vegetation growth. *Science Advances*, *5*(8), eaax1396.

Zhang, P., Jeong, J. H., Yoon, J. H., Kim, H., Wang, S. Y. S., Linderholm, H. W., Fang, K., Wu, X., & Chen, D. (2020). Abrupt shift to hotter and drier climate over inner East Asia beyond the tipping point. *Science*, *370*(6520), 1095–1099.

Zhou, S., Zhang, Y., Williams, A. P., & Gentine, P. (2019). Projected increases in intensity, frequency, and terrestrial carbon costs of compound drought and aridity events. *Science Advances*, *5*(1), eaau5740.

Zhu, Z., Piao, S., Myneni, R. B., Huang, M., Zeng, Z., Canadell, J. G., Ciais, P., Sitch, S., Friedlingstein, P., Arneth, A., Cao, C., Cheng, L., Kato, E., Koven, C., Li, Y., Lian, X., Liu, Y., Liu, R., Mao, J., … Cao, C. (2016). Greening of the Earth and its drivers. *Nature Climate Change*, *6*(8), 791–795.

Zohner, C. M., Mo, L., Renner, S. S., Svenning, J. C., Vitasse, Y., Benito, B. M., Ordonez, A., Baumgarten, F., Bastin, J. F., Sebald, V., Reich, P. B., Liang, J., Nabuurs, G. J., de Miguel, S., Alberti, G., Antón-Fernández, C., Balazy, R., Brändli, U. B., Chen, H. Y. H., … Crowther, T. W. (2020). Late-spring frost risk between 1959 and 2017 decreased in North America but increased in Europe and Asia. *Proceedings of the National Academy of Sciences of the United States of America*, *117*(22), 12192–12200.

Zscheischler, J., Mahecha, M. D., Harmeling, S., & Reichstein, M. (2013). Detection and attribution of large spatiotemporal extreme events in Earth observation data. *Ecological Informatics*, *15*, 66–73.

Zscheischler, J., Martius, O., Westra, S., Bevacqua, E., Raymond, C., Horton, R. M., van den Hurk, B., AghaKouchak, A., Jézéquel, A., Mahecha, M. D., Maraun, D., Ramos, A. M., Ridder, N. N., Thiery, W., & Maraun, D. (2020). A typology of compound weather and climate events. *Nature Reviews Earth & Environment*, *1*, 333–347.

SUPPORTING INFORMATION

Additional supporting information can be found online in the Supporting Information section at the end of this article.

How to cite this article: Yang, H., Munson, S. M., Huntingford, C., Carvalhais, N., Knapp, A. K., Li, X., Peñuelas, J., Zscheischler, J., & Chen, A. (2023). The detection and attribution of extreme reductions in vegetation growth across the global land surface. *Global Change Biology*, *29*, 2351–2362. https://doi.org/10.1111/gcb.16595